Colloids and Surfaces A 546 (2018) 168–178

Contents lists available at ScienceDirect

Colloids and Surfaces A

journal homepage: www.elsevier.com/locate/colsurfa

Surface Physicochemical and Structural Analysis of Functionalized Titanium Dioxide Films

Luciana D. Trino[a,*], Erika S. Bronze-Uhle[a], Anne George[b], Mathew T. Mathew[c], Paulo N. Lisboa-Filho[a]

[a] São Paulo State University (Unesp), School of Sciences, Bauru, SP, 17033-360, Brazil
[b] Department of Oral Biology, College of Dentistry, University of Illinois at Chicago, Chicago, IL, 60612, USA
[c] Department of Biomedical Sciences, College of Medicine at Rockford, University of Illinois-School of Medicine at Rockford, Rockford, IL, 61107-1897, USA

GRAPHICAL ABSTRACT

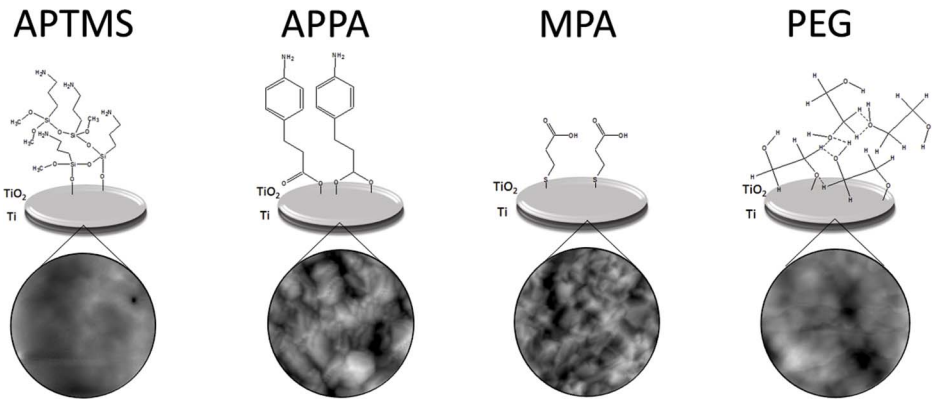

ARTICLE INFO

Keywords:
functionalization
titanium dioxide
thin films
physicochemical properties
adhesion mode
functional materials

ABSTRACT

Titanium and its alloys are recognized as acceptable materials for many applications. The properties of titanium dioxide (TiO_2) thin films are directly related to the structural characteristics of the material, which can be modified with tailor-made functional groups. Reactive bifunctional groups can be bound with hydroxyl-terminated TiO_2, leading to the formation of self-assembled monolayers or multilayer films. The understanding of such interactions is necessary to design functional oxide coatings for a large variety of applications. In this study, nanosized TiO_2 films were synthesized by the sol-gel method and deposited by spin coating technique upon titanium substrate. Subsequently, TiO_2 thin films were functionalized with (3-aminopropyl)trimethoxysilane (APTMS), 3-(4-aminophenyl)propionic acid (APPA), 3-mercaptopropionic acid (MPA) or polyethylene glycol (PEG). Surface characterization by XPS, surface roughness, and contact angle indicated successful functionalization and allowed for identification of the preferential conformation of each molecule. APPA and APTMS presented free amine groups indicating the attachment to the surface by carboxyl and silane groups, respectively. Mercapto coupling from MPA showed the formation of S-Ti bonds. PEG-coated surface revealed polymerization of several hydroxyl groups that crosslinked with each other. Analyzing the mode of attachment at the interface of the metal oxide and functional group may help in the development of improved functional materials.

* Corresponding author.
E-mail address: lucianatrino@fc.unesp.br (L.D. Trino).

https://doi.org/10.1016/j.colsurfa.2018.03.019
Received 11 January 2018; Received in revised form 20 February 2018; Accepted 6 March 2018
Available online 07 March 2018

1. Introduction

Titanium dioxide (TiO_2) thin film is well known for its optical [1], photocatalytic [2], anti-corrosive [3,4], and antimicrobial properties [5]. It has been applied in paint coatings, as well as in the fields of energy, environment, and biomaterials [6–8]. The properties of TiO_2 films are directly related to the structural characteristics of the material, which can be tailored by the synthesis, deposition, or annealing method. The technique employed can influence the particle size, morphology, crystalline phase, thickness, roughness, wettability, and surface chemistry, and consequently its application. There are many different routes for the formation of titania thin films, including vacuum evaporation, sputtering, electrodeposition, Langmuir-Blodgett technique, and the sol-gel process [9]. Among these methods, sol-gel routes are considered to be the simplest. These routes present the possibility of homogeneity and microstructure control, as well as lower energy consumption, since the process is usually conducted at lower temperatures than those used in the conventional synthesis of ceramics [10]. The type of precursor, acidic or basic catalyst, and the temperature in the hydrolysis step determines the nature and properties of the products [11]. A high molar ratio of water effectively dilutes the alkoxide and accelerates the hydrolysis step leading to the formation of nanosized particles [12,13]. In general, the sol-gel product is deposited on a substrate by spin or dip-coating. The spin coating technique is a simple method that offers the advantages of low cost, the ability to form particles with good size distribution, control of the film thickness, reproducibility of the process, and the ability to provide highly uniform coatings [10].

The functional properties of titania thin films may be improved through surface modifications to suit various applications. Currently, there has been an increasing interest in the formation of chemically modified oxide surfaces with organic functionalities [14,15]. Hybrid surface architectures combining active organic and inorganic components at the nanometer scale play a crucial role in the development of functional materials [16,17], and these could be considered as self-regulating “intelligent” surfaces [18]. For these systems, the control of organic/inorganic interfaces and the creation of strong linkages between the different elements through covalent or ionic bonds can lead to remarkable properties due to synergistic effects [19]. The oxidized surface facilitates the strong adhesion of reactive functional groups (-SH, -COOH, $-NH_2$, etc.) yielding surfaces with great stability and functionality.

The organic molecules may adsorb on the TiO_2 surface by physisorption or covalent bond formation. The presence of hydroxyl groups (-OH) on the titania surface, under ambient conditions, leads to the formation of covalent interactions between -OH and a specific functional group from the organic molecules through condensation reactions [20]. The covalent interaction between the substrate and the organic moieties depends on the reaction conditions and the type of functional groups present on the organic compound. Generally, the organic molecules that will interact with TiO_2 have two functional groups. The functional group with higher affinity for the substrate, the headgroup, interacts covalently with the -OH surface groups. The other terminal functional group will be free to interact with other molecules on the surface, such as peptides or proteins that are useful for bio-applications. Furthermore, the terminal group will be additionally responsible for the characteristics of the organic interface, which will define the surface properties [21].

There are two approaches normally used for surface functionalization: the deposition of multilayers; or the attachment of self-assembled monolayers (SAMs) [20,22]. SAMs result in ordered, oriented, and packed layers of organic molecules formed on the surface by equilibration to a structure of minimum surface free energy [23]. Multilayers result in disordered layers due to uncontrolled growth arising from fast reactions or interactions. Both these methods have their advantages and disadvantages. Monolayers provide a high level of control over the molecular level composition. However, the degree of order in these systems is largely determined by the alkyl chain length [24]. Furthermore, there are many parameters that can influence the preferential formation of a single or multilayer, such as deposition time, adsorption mechanisms, and molecular architectures. Thus, it is necessary to gain a better understanding of the type of attachment and growth mode at the interface, along with the functional group/metal oxide combined with surface-sensitive and bulk characterization techniques.

In this study, we describe our investigations of TiO_2 rutile sol-gel synthesis and deposition upon titanium substrates in order to form a nanostructured thin film, which is further modified with bifunctional groups to form hybrid functional materials. Titanium dioxide thin films were functionalized with four different organic bifunctional molecules in order to better understand the mechanism behind mercapto, amine, carboxyl, and hydroxyl group attachment. The morphology, roughness, and surface chemistry of the oxide influences the adhesion, conformation, and growth mode of the organic molecules. A surface sensitive technique such as X-ray photoelectron spectroscopy (XPS) was combined with contact angle measurements, atomic force microscopy (AFM), scanning electron microscopy (SEM), and X-ray diffraction (XRD) to gain a deeper insight into the formation of these functional materials and to understand the adhesion mechanisms.

2. Materials and Methods

2.1. Oxide Synthesis

Titanium dioxide solution was synthesized by a sol-gel route. The synthesis occurred by hydrolysis and condensation reaction of the titanium isopropoxide (IV) employing a high molar ratio of water:-alcoxide (200 : 1), isopropanol as co-solvent, nitric acid (HNO_3) as a catalyzer and Triton X-100 as a surfactant. Distilled water (185 mL) was mixed with isopropanol (56.7 mL, Merck) and nitric acid (2.6 mL, Synth). Then, titanium isopropoxide (IV) (15 mL, Aldrich) was added and the mixture stirred for 30 min. Subsequently, the peptization was initiated covering the reaction beaker and heating the solution at 85 °C under magnetic stirring for four hours. During this step, the evaporation of the solvents during hydrolysis results in the condensation of the colloid, which presented a light translucent blue color. In order to form the gel phase, the solution was kept under heat and stirred until a final volume of 50 mL was reached, and the solution presented a milky-white color. Finally, Triton X-100 surfactant (0.816 g, Synth) was added to 50 mL of the solution and stirred for15 min.

2.2. Substrate Preparation

Commercial pure titanium discs (15 mm diameter x 3 mm thickness) were polished until Ra ≈ 150 nm and then cleaned with isopropanol and deionized water for 15 minutes each in an ultrasonic bath. The samples were etched and hydroxylated in Piranha solution (a mixture of 7:3 (v/v) 98 % H_2SO_4 and 30 % H_2O_2) for two hours. After that, the substrates were rinsed copiously by deionized water for immediate oxide deposition.

2.3. Oxide Deposition

The deposition was performed by spin coating technique (2000 RPM per 60 seconds), the procedure was repeated three times for each sample. Between the depositions, the samples were heated for five minutes on a hot plate at 40 °C. After that, the samples coated with TiO_2 oxide were annealed at 850 °C for two hours in a heating rate of 1 °C min^{-1} in order to obtain a rutile crystalline polymorphic phase.

2.4. Organic Molecules Deposition

TiO_2 surface was functionalized with four different bifunctional molecules: (3-aminopropyl) trimetoxysilane (APTMS, Aldrich), 3-(4-

aminophenyl)propionic acid (APPA, Aldrich), 3-mercaptopropionic acid (MPA, Aldrich) and polyethylene glycol (PEG, Synth). The samples functionalization occurred by the immersion method as described below.

2.4.1. 3-(4aminophenyl)propionic acid

APPA solution (2 mM) was prepared in ethanol absolute (Merck) by stirring the solution on the magnetic plate for 5 minutes. After complete dissolution, it was heated up to 40°C, and then the substrate was immersed for 5 minutes.

2.4.2. (3-aminopropyl)trimethoxysilane

APTMS solution (10 mM) was prepared in ethanol (Merck) and the substrate was immersed in the solution for 1 minute at ambient temperature.

2.4.3. 3-mercaptopropionic acid

An aqueous solution (1 mM) was prepared with MPA adjusting the solution pH to 3 with HCl (Synth). The samples were immersed for 10 minutes in the solution under ambient temperature.

2.4.4. Polyethylene glycol

A mixture of the ratio of PEG (1 g, MW 8000) and distilled water (4 mL) was prepared. PEG was diluted, and the substrates were added to the solution and kept overnight. The samples were rinsed with water after the immersion.

After the deposition of the organic molecules, all samples were dried overnight at ambient conditions.

2.5. Characterization

2.5.1. X-ray Diffraction (XRD)

The crystalline orientation of TiO_2 films was measured under ambient temperature using an X-ray diffractometer system (D/MAX-2100/PC, Rigaku), which employs the CuKα radiation (1.54056 Å) coupled to a nickel filter, in order to eliminate the CuKβ radiation. The applied tension was 40 kV, and the current was 20 mA. The scanning range was from 20 ° to 45 °, with the regular step of 0.02 ° min^{-1} and scan speed of 2 ° min^{-1}. In order to determine the crystal structure, the results were compared with PCPDF 76-1949 card.

2.5.2. Scanning Electron Microscopy (SEM)

Structural characterization of the films was performed by Scanning Electron Microscopy (FEG-SEM JEOL 7500F). For cross section images, the oxide layer was deposited on a silicon substrate coated with Ti, under the same conditions as previously described for titanium substrates. A diamond cutter was used to cut the Si-Ti substrate coated with TiO_2 from the backside of the sample. The samples were coated with gold and mounted on an aluminum stub with a double-sided conductive carbon tape for imaging the surface and the cross section of the samples. The measurements were performed applying a voltage of 2.00 kV and a working distance of 8 mm.

2.5.3. Confocal Microscopy

Surface roughness characterization was performed by confocal microscopy (Leica DCM3D) employing a 20 x lens. Roughness values (RMS) were determined by calculating the mean value from six randomly selected areas for each sample.

2.5.4. Atomic Force Microscopy (AFM)

AFM images were analyzed by the non-contact model using an atomic force microscope (Veeco), model Nanoscope III. The tips used were probe model FESP by Veeco Instruments, with 8 mm of curvature radius and 75 kHz resonance frequency.

2.5.5. Surface Contact Angle

The contact angle and surface energy were evaluated by the sessile drop technique in a goniometer (Ramé-Hart, 100-00) and using deionized water (polar substance), and diiodomethane (non-polar substance) as the probing liquids. At least three droplets were deposited on different positions of the samples and contact angle was measured at each side of the drop. Measurements were performed at room temperature and under controlled humidity environment. The contact angle and surface energy were evaluated by DROPimage software on the basis of the Young-Laplace equation describing the drop profile of sessile drops. More specifically, calculation of surface tension was done by means of a method based on a least squares fit to theoretical profiles produced by a numerical integration of the Young-Laplace equation [25].

2.5.6. X-ray Photoelectron Spectroscopy (XPS)

To determine the chemical states of the elements, the analysis was carried out in a Kratos (AXIS-165) using a monochromatic Al Kα X-ray source. After prepared, the samples were stored in a vacuum desiccator at a maximum period of 24 h before the XPS measurements. The XPS measurements were done without Ar cleaning and the samples were kept overnight inside the equipment to reach the desired vacuum of the system. Each sample was analyzed at take-off angle, defined as the angle of emission relative to the surface, of 54.7 °. The energy resolution was 0.45 eV. Survey scan spectra were recorded at a pass energy of 80 eV, and individual high-resolution spectra at a pass energy of 20 eV. In order to correct for any charging effect, the binding energy of the C 1s peak was normalized to 285 eV, referred to the C 1s line of the carbon contamination. Curve fitting was performed using the CasaXPS software using as line shape GL(30) mode and with a FWHM constriction between 0.7 and 2.5 eV. Peak identification was done to obtain a consistent fit for all the potentials investigated.

3. Results and Discussion

3.1. TiO_2 sol-gel synthesis: reaction mechanism

By using a sol-gel process, the synthesis of titanium dioxide can be independently performed with inorganic or organic precursors, obtaining a monodisperse and submicron TiO_2 powder.

A common method for obtaining TiO_2 nanoparticles is to hydrolyze an alkoxide precursor, $Ti(OR)_4$, where R is an organic radical, using sub-stoichiometric hydrolysis ratios and inorganic acid catalysts (HCl, HNO_3) [11]. Through this organic process, the reactions involved may be represented in two steps: hydrolysis and condensation. In addition, the amount of water directly influences the reaction-condensation, which is competitive with alkoxolation, oxolation, or olation, changing the tridimensional polymer backbone to be obtained [26].

The first step consists of the hydrolysis of the alkoxide precursor (Fig. 1), which occurs in the presence of water leading to the formation of Ti-OH bonds. A large amount of water effectively thins the alkoxide and accelerates the hydrolysis step. Under these conditions, nanosized particles are formed [12]. The subsequent step involves condensation reactions, during which there is a preferential transformation of $Ti(OH)_4$ in $Ti(OH)_4O^+H_2$ species through a solvation phenomenon [26]. The presence of reactive species Ti-HO^+-Ti may contribute to the development of polymer chains of Ti-O-Ti through olation reaction [27]. The olation occurs by a nucleophilic substitution process wherein M-H is the nucleophile and M is Ti^{4+}. Through the nucleophilic substitution, the removal of the aqueous binder (H_2O^+) from the coordination sphere occurs in reactions with an excess of water. Alternatively, in the presence of alcohol as a co-solvent, the removal of R-OH species occurs. Thus, the binding lability for M-OH_2 or M-OHR determines the kinetics of the olation reaction.

The process is continued by peptization, which constitutes the redispersion of the colloid by breaking the aggregates and forming a

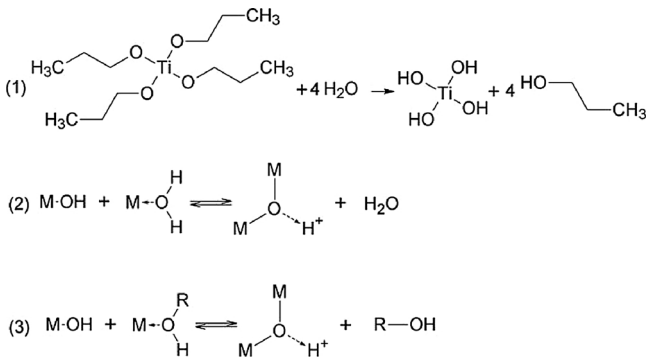

Fig. 1. Sol-gel reaction mechanisms. (1) Hydrolysis of the titanium isopropoxide; Nucleophilic substitution by olation reaction in (2) excess of water and (3) presence of co-solvent.

translucent sol containing small particles distributed over a narrow range of sizes. This occurs in the presence of an acid medium, on which H_3O^+ ions act as peptizing ions ensuring high surface charges on the particles for their separation. Finally, as the solvent evaporates, it starts forming a three-dimensional network gel, through the adhesion of sol phase particles. The surfactant plays an important role in the size distribution of the particles and in the adhesion of the film.

3.2. TiO_2 thin film characterization

The TiO_2 thin films were analyzed by X-ray diffraction (XRD). A representative result is shown in Fig. 2a. A pronounced (110) peak of TiO_2 at $2\theta = 27.7^\circ$ was observed, indicating the presence of the rutile polymorphic phase. Other characteristic diffraction peaks from rutile TiO_2 were observed at 36.3°, 39.4°, 41.5°, and 44.3° in a 2θ range between 20.0° and 45.0°. Two weak diffraction peaks appeared at approximately 25.0° and 40.0°, which are attributed to the anatase (PCPDF 89-4921) and titanium (PCPDF 44-1294) crystal phases, respectively. The titanium phase peak is originated from the Ti substrate. Due to the thin oxide film deposited, some X-rays from the substrate were detected. These results indicate that the TiO_2 thin films are mainly composed of rutile crystals of TiO_2, which is known to be more inert and resistant to corrosion than the anatase phase, and can improve the wear resistance of the material due to its self-lubricating properties [28].

The TiO_2 surface was analyzed by SEM. The oxide presented a granular and rough structure with sintered particles due to the high annealing temperature (Fig. 2b). However, no defects were observed. An average TiO_2 particle size was estimated by Image J software. The value obtained was around 75 (± 6.4) nm.

Cross-section SEM images showed a good adhesion at the interface between the titanium substrate and the TiO_2 film (Fig. 2c), in agreement with the pull off test (Fig. S1). A titanium surface normally does not have enough intrinsic hydroxyl groups for covalent bonding with TiO_2. To overcome this, piranha etch, a strong oxidizer, provided a hydroxylated surface making it extremely hydrophilic to bond with the TiO_2 thin film. Furthermore, the TiO_2 thin film thickness was around 500 nm, which was controlled by the precursor solution viscosity and the rotating speed.

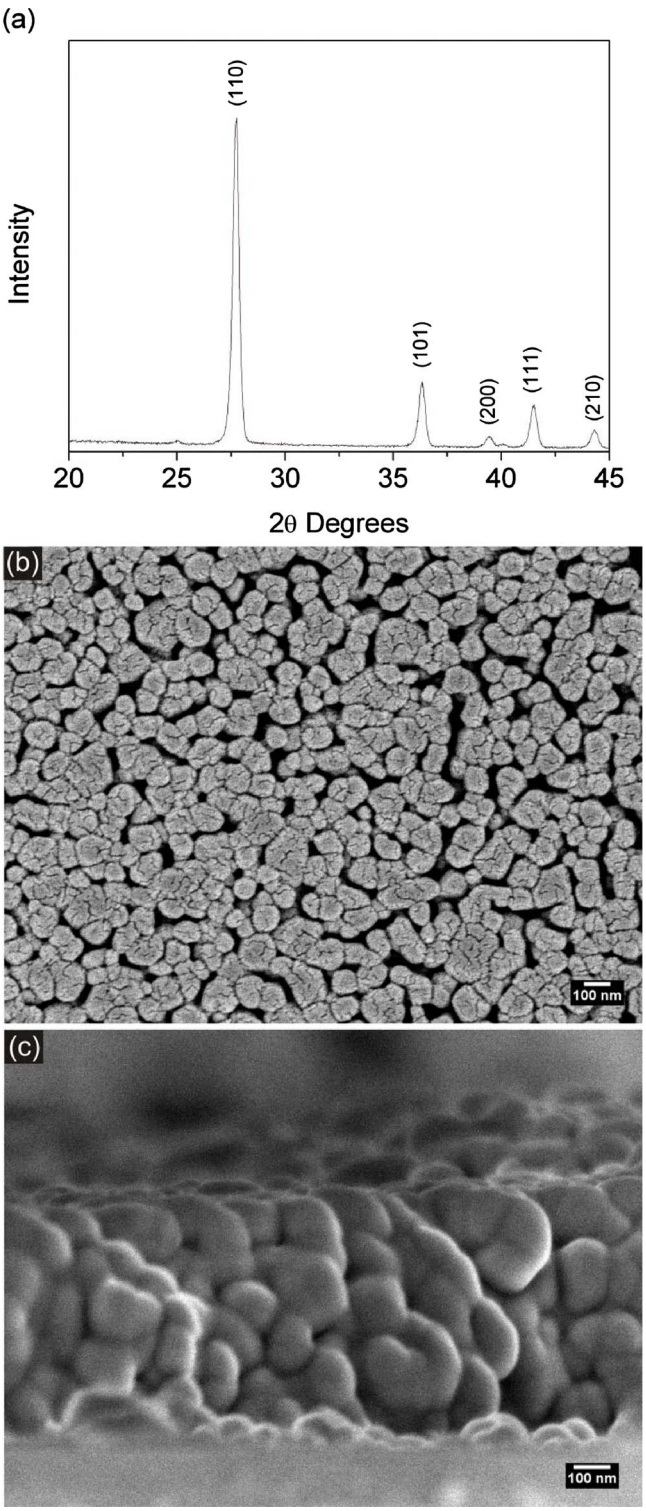

Fig. 2. Characterization of the TiO_2 rutile thin film by XRD spectrum (a), and by SEM images for TiO_2 top surface (b) and cross-section (c).

3.3. Surface functionalization with bifunctional molecules

The physicochemical characteristics of different functional groups were evaluated to analyze the chemical attachment, surface roughness, and surface energy from the interfaces. The bifunctional chemical compounds analyzed were: 3-(4-aminophenyl)propionic acid (APPA, $H_2NC_6H_4CH_2CH_2CO_2H$); (3-aminopropyl)trimethoxysilane (APTMS, $H_2N(CH_2)_3Si(OCH_3)_3$); 3-mercaptopropionic acid (MPA, $HSCH_2CH_2CO_2H$); and polyethylene glycol (PEG, $H(OCH_2CH_2)_nOH$).

The AFM images (Fig. 3) show a comparison of the surface topography for the various samples analyzed. Fig. 3a shows the pristine Ti surface with small particles and some defects resulting from the polishing process. The rutile TiO_2 surface is characterized by larger and homogeneously dispersed grains (Fig. 3b). The AFM images show a homogenous surface coverage for the APPA and MPA molecules, indicated as small white dots on the TiO_2 grain boundaries (Fig. 3c and e). The adhesion of APPA and MPA molecules onto the titanium dioxide

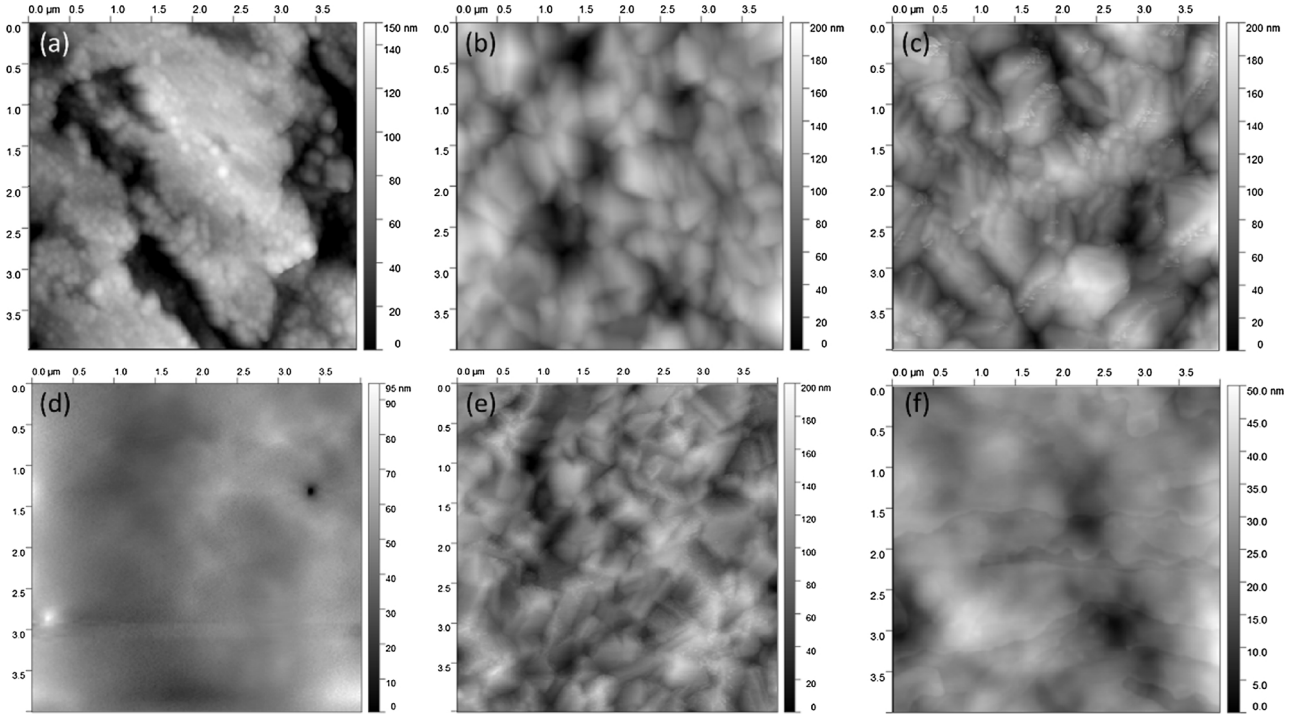

Fig. 3. AFM images for pristine Ti (a), TiO_2 (b), TiO_2 APPA (c), TiO_2 APTMS (d), TiO_2 MPA (e) and TiO_2 PEG (f).

surface may occur through the TiO_2 grain boundaries due to the higher surface energy in those regions. By contrast, APTMS and PEG showed the formation of multilayers, characterized by a dense deposition on the surface on which the metal oxide nanoparticles were completely covered (Fig. 3d and f).

In the case of APTMS, the formation of multilayers can be explained in terms of the nature of the solvent. Regarding non-anhydrous ethanol, the presence of water leads to a much faster condensation reaction not only with the surface hydroxyl (-OH) groups, but also with neighboring silanol groups [20,29]. This may yield disordered inhomogeneous multilayers. PEG molecules, however, have several hydroxyl groups that can crosslink themselves to form a multilayer.

Fig. 4 shows changes in the root mean square (RMS) surface roughness of the pristine Ti substrate, TiO_2 thin film, and the functionalized oxide thin films. The pristine Ti surface roughness is around 180 (± 31) nm. After being coated with TiO_2 thin films, there is an increase in RMS to 376 (± 32) nm, and sharp peaks can be discerned from the TiO_2 confocal image. There was no statistical difference between the samples of pristine TiO_2, TiO_2 APTMS (380 ± 12 nm), TiO_2 MPA (338 ± 27 nm), and TiO_2 PEG (364 ± 7 nm). The TiO_2 APPA sample indicated a minimum decrease in RMS to 314 (± 7) nm. The difference in surface roughness between pristine TiO_2 and the functionalized samples with all the organic molecules analyzed was less than 50 nm. Comparing the surface roughness data with the schematic models of attachment (Fig. 8), we can assume that even with a multilayer formation, in the case of APTMS and PEG, a thin layer of organic molecules is formed upon the TiO_2 surface. In the case of TiO_2 APPA, the organic molecules probably adhered to the surface in the valley regions, showing a slight decrease in RMS.

To further evaluate the adhesion process of the bifunctional molecules on TiO_2 surfaces, the surface wettability of the as-obtained functionalized TiO_2 thin films was assessed by water contact angle (CA) and surface energy (SE) measurements. The wettability properties of the surface functionalized TiO_2 thin films were expected to vary from the pristine TiO_2 films and Ti substrates due to the different functional terminal groups present on their surfaces. Fig. 5 shows the water CA and SE for the controls (Ti and TiO_2) and functionalized samples. Pristine Ti presented a CA of 72(± 2.0)°. The surface modification with TiO_2 thin film increased the wettability of the material due to the presence of terminal hydroxyl groups, showing a CA of 67(± 2.4)°. In

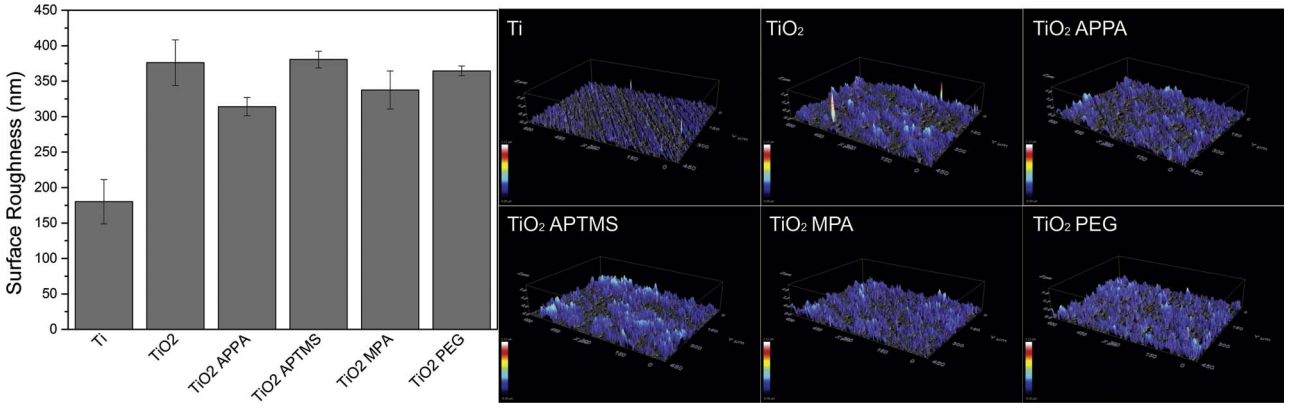

Fig. 4. Surface roughness average for the functionalized samples.

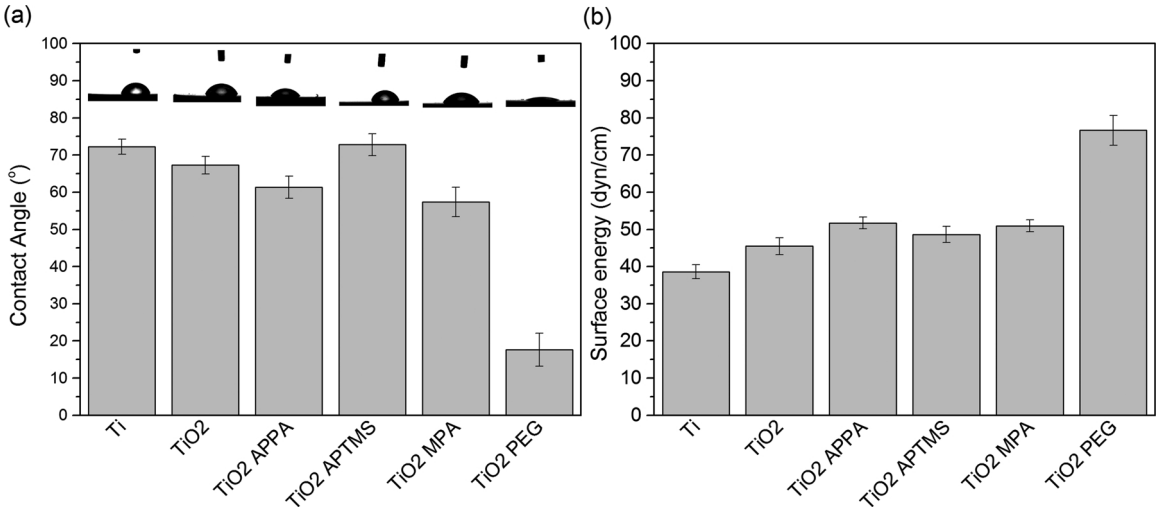

Fig. 5. Contact angle (a) and surface energy (b) values for the control (Ti and TiO_2) and the functionalized samples, indicating higher wettability, except for APTMS, and increased surface energy for the functionalized surfaces.

general, the functionalization of TiO_2 led to an increase in hydrophilicity of the material. The TiO_2 APPA sample showed a slight enhancement in hydrophilicity, with a CA of 61(± 3.0)°. The surface wettability for the TiO_2 MPA sample increased, which can be verified by the CA of 53(± 4.0)°. The major difference in CA value was observed for the TiO_2 PEG sample (18(± 4.4)°), which tailored the surface with higher hydrophilic properties. This behavior can be attributed to the existence of oxygen in the backbone -(CH_2CH_2O-)n [30] and to the long carbon chain that interacted randomly on the surface, contributing to the acquisition of a very smooth and highly hydrophilic surface [31]. The only exception was TiO_2 APTMS; this material showed a moderate contact angle of 73(± 2.9)° and a more hydrophobic behavior over the other functionalized samples.

The outermost layer predominantly controls the wettability of surface functionalized TiO_2 thin films [32], suggesting that surface functionality treatment on TiO_2 thin films was successfully achieved. Furthermore, the surface functionalization led to an increase in SE. Titanium surfaces tend to have low surface energy (39 ± 2.9 dyn/cm) [33]. However, with the deposition of TiO_2 thin film, a slight increase to 45 (± 2.3) dyn/cm was observed. A considerable difference in SE was noticed on the functionalized samples, due to the presence of reactive terminal groups. The TiO_2 APPA and TiO_2 MPA samples showed a similar SE value of 52 (± 1.6) dyn/cm and 51 (± 1.7) dyn/cm, which can be attributed to the amine (-NH_2) and carboxylic acid (-COOH) free groups, respectively. Besides the more hydrophobic behavior, the TiO_2 APTMS sample exhibited a higher surface energy (49 ± 2.2 dyn /cm), when compared to the control samples, due to the presence of free -NH_2 groups on the surface. The higher surface energy was observed for TiO_2 PEG (77 ± 4.0 dyn/cm). The presence of several hydroxyl groups increases TiO_2 PEG polarity and subsequently enhances the ability to interact with the approaching water molecules.

Both micro and nanoscale surface roughness, as well as chemical functionalities, play an important role in wettability of materials, primarily in the fields of biomaterials and engineering surfaces [34–38]. Although the functionalized samples had similar RMS values, even small increments in surface roughness could lead to an enhanced wettability caused by the chemistry of the surface [39]. In this way, the surface roughness contributed to the TiO_2 PEG sample's hydrophilic behavior, as well as to the more hydrophobic performance observed for the TiO_2 APTMS sample. Whereas the RMS, CA, and SE values were similar to TiO_2 APPA and TiO_2 MPA samples, it is assumed that the major influence in wettability was caused by the chemical functionalities for these samples. Furthermore, these results show that the physicochemical nature of TiO_2 surfaces can be easily controlled via functionalization.

X-ray photoelectron spectroscopy (XPS) experiments were used to examine the adsorption of amine, silane, mercapto, carboxyl, and hydroxyl groups on a titania surface. The obtained XPS results showed an increase in the intensity of C 1s (285 eV) for all functionalized samples when compared with the sample coated with only TiO_2 (Fig. 6a), followed by the presence of the elements N, S, and Si, indicating the success in the functionalization process in accordance with CA measurements. Different contributions of oxygen can be observed in the high-resolution spectrum of O 1s from the TiO_2 specimen (Fig. 6b), which can be divided into three peaks. The first two peaks, located at lower energy levels, are typical for the metal oxide bonds in TiO_2 [40]. The third peak, located at 531.4 eV, is assigned to the oxygen of Ti-OH bonds [41]. Fig. 6c shows the high-resolution spectrum for Ti 2p. The energy difference between spin-orbit peaks Ti 2p1/2 and Ti 2p3/2 is 5.7 eV, which is consistent with Ti^{4+} in the TiO_2 bond [42]. From fitting data, the full width at half maximum (FWHM) for Ti 2p is 0.970 for Ti 2p3/2 and 1.862 for Ti 2p1/2. The FWHM for metals are usually less than for oxides, which is probably the reason for this unusual difference. The XPS results for TiO_2 proved that the surface contains hydroxyl groups that act as anchoring points for the formation of densely packed mono or multilayers.

3.4. Mode of attachment

The preferential attachment of APTMS, APPA, MPA, and PEG on a TiO_2 surface is described based on the high-resolution XPS spectra for each sample, as shown in Fig. 7. APTMS has an amine and a silane group, making it able to attach from both sides on the TiO_2 surface. From analyzing the XPS peaks it is evident, particularly from N 1s and O 1s, that APTMS molecules were bonded on the titanium dioxide surface. Several specific features are apparent that allow further conclusions on the covalent bond formation and molecular conformation upon attachment. In the N 1s spectrum (Fig. 7a), a small broad peak at 397.8 eV assigned to N-Ti bond is observed [43], indicating that a small amount of APTMS molecules might be bonded through amine groups. However, a sharp and intense peak at 399.4 eV is attributed to NH_2, while another one at 401.2 eV is related to the C-N bond [40]. These results indicate a preferential attachment of APTMS molecules through silanization, because when silane coupling occurs, free NH_2 groups are observed [44]. Furthermore, if the reverse attachment occurred it would lead to an N 1s peak at 400.9 eV, and this was not observed.

The attachment through silanization can also be confirmed by O 1s spectrum (Fig. 7b), which shows contributions from five different species. The first two are related to titanium bonded with oxygen in TiO_2.

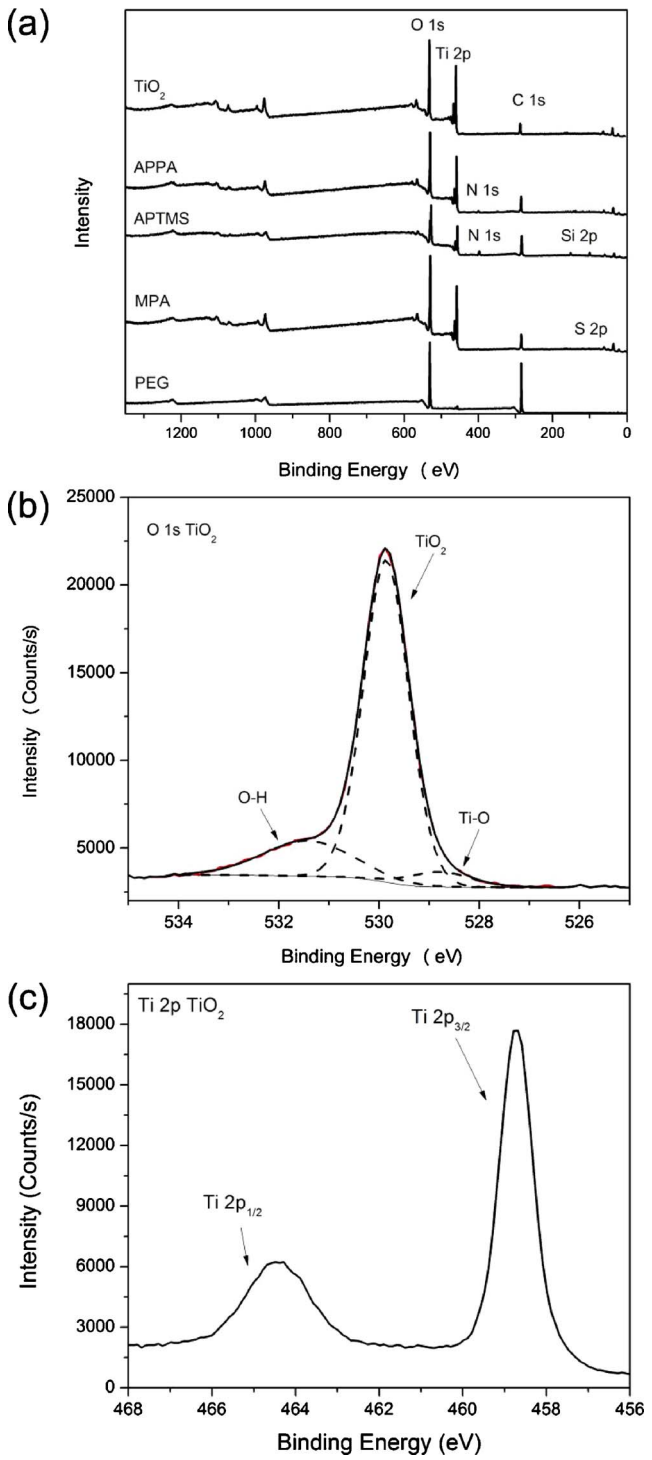

Fig. 6. XPS survey spectrum of the samples analyzed (a); high-resolution O 1s spectrum (b) and Ti 2p spectrum (c) for the prepared TiO_2 films.

At an energy of 531.3 eV, it is possible to observe Ti-O-Si species [45] that are formed after the silanization process. The two peaks at higher energy can be attributed to O-Si-O (532.7 eV) and Si-OH (534.4 eV) species [40]. The APTMS mechanism of attachment occurs first by silane hydroxylation; then the Si-OH can quickly react by condensation and form Si-O-Si groups with the surface hydroxyl groups and neighboring silanol groups. Formation of such covalent bonds between silanes and the underlying substrate stabilizes the monolayer [20]. The presence of water leads to a much faster condensation reaction which can yield multilayers, as observed by AFM.

Grafting of APPA molecules upon the TiO_2 surface can occur either by carboxylic acid or amine groups. The N 1s spectrum (Fig. 7c) shows the contribution from C-N (400.1 eV) and NH_3^+ (401.2 eV) species [40]. The presence of NH_3^+ suggests that it could be generated by the formation of a zwitterionic amine structure favoring the adsorption through the carboxylate group [46–48]. The absence of an N-Ti bond indicates no surface interaction between the titanium dioxide and nitrogen. Another feature that supports this conclusion of APPA attachment through the carboxyl is the presence of COO- species (288.8 eV) in C 1s spectrum after APPA attachment (Fig. 7d) [49].

Furthermore, the solution pH and the acidic or basic properties of the oxide play an important role in bonding with organic molecules. The oxide layer provides a pH on which the positive and negative charges resulting from the hydroxyl group's dissociation in solution are balanced, and the apparent charge is zero. This pH value is known as the point of zero charge (pzc). In the case of rutile TiO_2, the pzc is 5.3 and the APPA solution pH is 6.4 [50]. It means that at a pH higher than 5.3, the TiO_2 surface is slightly basic and the APPA molecules have a preferential attachment through the carboxyl groups, which corroborates the XPS results.

In addition, the attachment of MPA molecules can succeed through mercapto or carboxylic acid groups upon the TiO_2 surface. Regarding the rutile TiO_2 pzc and MPA solution pH, the bonding with MPA molecules would be expected to occur through the mercapto groups. Since the pH of the MPA solution is equal to 3 (lower than 5.3), it leaves the oxide surface with acidic characteristics leading to a preferential attachment by the mercapto groups. In the C 1s spectrum (Fig. 7f), three components are observed: the first one at lower energy is related to the C-C bond in the MPA molecule (284.9 eV); a contribution at 285.8 eV is associated with the C-S bond; and at higher energy (288.6 eV), it can be attributed to the presence of COOH [40]. The high resolution sulfur spectra exhibit several S 2p spin-orbit coupling (S 2p1/2 and S 2p3/2) at approximately 159, 164, and 168 eV. From the analysis of the S 2p spectrum, Fig. 7e, we can conclude that mercapto functional coupling occurs preferentially due to the presence of a doublet near 164 eV that is commonly assigned to the S-Ti bond [51], and another S 2p spin-orbit coupling assigned as $S\text{-}Ti^{+3}$ species at 159.7 eV [52]. Furthermore, at 168.8 eV it is observed that another doublet is assigned as S-O bond, which is associated with the hydroxyl groups present on the TiO_2 surface [51], corroborating the previous findings that MPA binds covalently with the TiO_2 surface through mercapto groups.

It is known that PEG has several hydroxyl groups available for derivatization. In O 1s spectrum (Fig. 7h) we can observe a small amount of O-Ti-O bond and O-H in 529.8 and 531.0 eV [40], respectively. A sharp and intense peak at 532.4 eV, assigned to $-CH_2\text{-}CH(OH\text{-})_n$, indicates the formation of a polymeric layer on the titania surface. The increase of C 1s and O 1s in the PEG treated surface followed by a decrease in Ti 2p intensity (Fig. 7g) might suggest that the hydroxyl groups present on PEG are cross-linked with each other by polymerization [53].

A schematic model based on the XPS and AFM analysis for the preferential attachment of the bifunctional molecules with the TiO_2 surface is shown in Fig. 8. As show by AFM, APTMS and PEG molecules formed multilayers (Fig. 8a and d), which attached to the TiO_2 surface by silane and hydroxyl groups, as confirmed by XPS. The XPS measurements indicated that the APPA and MPA molecules attached to the surface by carboxyl and mercapto groups, respectively. However, it was not possible to identify by AFM if they formed a mono- or multi-layers, in this way Fig. 8b and c may have more than one molecule of thickness.

Besides the thickness of the organic layer, due to the presence of different terminal groups on the surface, each bifunctional molecule modifies the TiO_2 physicochemical properties in a characteristic manner, which can be controlled depending on the required application. The studied organic molecules are classic examples of coupling agents that have widespread applications ranging from high-

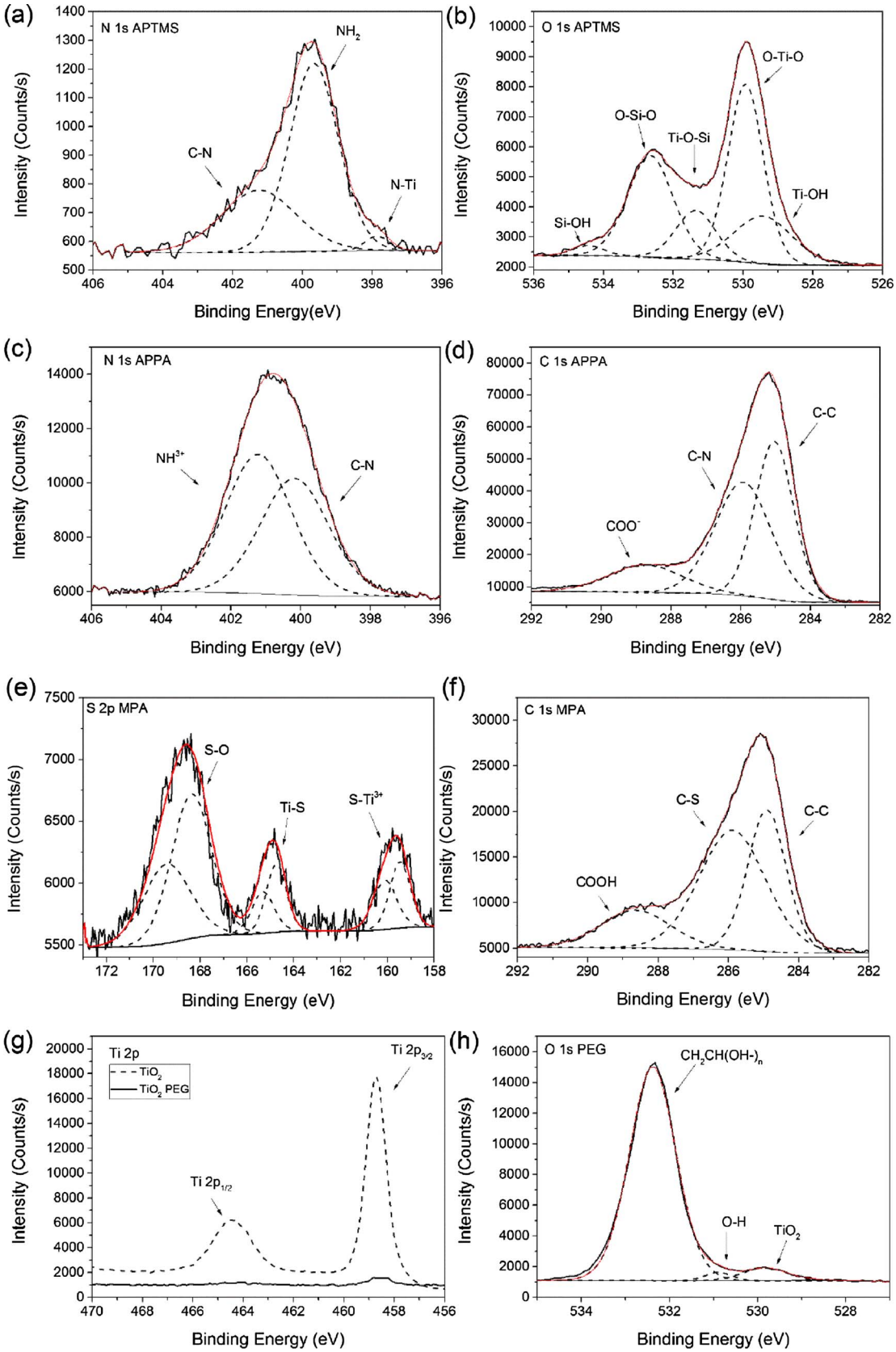

Fig. 7. XPS high resolution spectra for the elements present on APTMS, APPA, MPA and PEG molecules. For APTMS it is shown the N 1s (a) and O 1s (b) spectra which led to a possible orientation by silane groups; APPA N 1s (c) and C 1s (d) spectra indicated a preferential attachment through COOH group; MPA adhesion was analyzed in terms of S 2p (e) and C 1s (f) indicating that it occurs by mercapto group; Considering Ti 2p (g) and O 1s (h) spectra from PEG, this molecule exhibited a polymerization with free –OH groups.

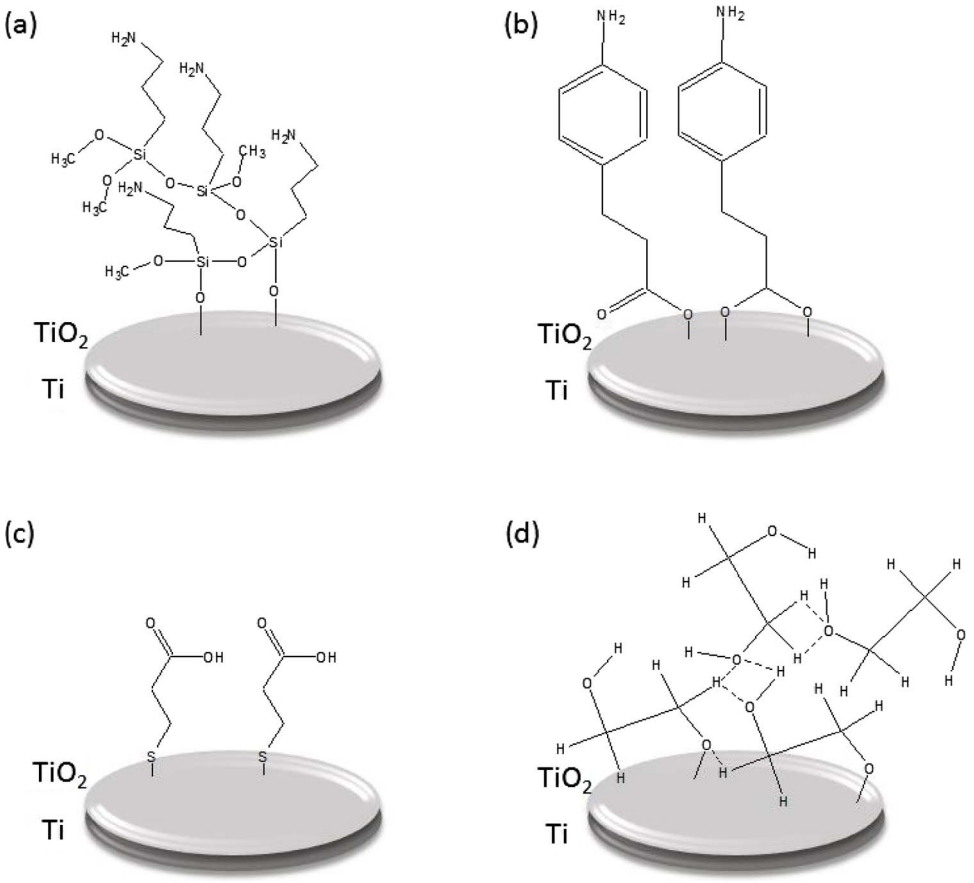

Fig. 8. Possible schematic model of attachment for the bifunctional molecules APTMS (a), APPA (b), MPA (c), and PEG (d) on TiO_2 surface. The APTMS adhered to the surface by silane groups that reacted fast by condensation with the surface and neighboring silanol groups, resulting in disordered inhomogeneous multilayers. The APPA molecules attached the surface preferentially through COOH group, in a mono or bidentate way forming mono- or multi-layers. The MPA adhesion occurs by mercapto group that may form mono- or multi-layers. In the case of PEG, this molecules cross-linked with each other by polymerization forming multilayers.

throughput cell culture platforms, biomedical devices, lab-on-a-chip, self-cleaning fabrics, anti-fog windows, to anti-corrosive coatings [18,20,37,54,55].

4. Conclusion

In this study, we characterized the surface morphological and physicochemical properties of TiO_2 thin films. These films were prepared by sol-gel synthesis with high water content in order to form a nanostructured thin film. Titanium dioxide thin films were in rutile crystalline polymorphic phase presenting a crystallite size of 75 (± 6.4) nm. Titania films were then functionalized with four different organic bifunctional molecules: APTMS, APPA, MPA, and PEG.

The AFM images showed an attachment through the grain boundaries region for APPA and MPA molecules, and a multilayer formation for APTMS and PEG molecules. The difference in surface roughness between pristine TiO_2 and the functionalized samples was less than 50 nm, showing that a thin layer of organic molecules was formed upon the TiO_2 surface. In general, the functionalization of TiO_2 led to an increase in hydrophilicity of the material, except for APTMS molecules, which is related to surface roughness. Small increments in surface roughness can lead to an enhanced wettability caused by the chemistry of the surface. Overall, the surface energy increased after functionalization. The higher surface energy was observed for TiO_2 PEG due to the presence of several hydroxyl groups that enhance the ability to interact with the approaching water molecules.

Moreover, by the photoelectron experiments, there was proposed possible adhesion mechanisms and a growth mode of the organic molecules. The results confirmed that APTMS has a preferential attachment upon TiO_2 surface through silane groups due to the formation of a covalent bond between silanes and the underlying substrate. However, the presence of water led to the formation of multilayers. APPA grafting favored a covalent bond with the TiO_2 surface through the carboxylic acid group, presenting free amine groups and the absence of an N-Ti bond. The mercapto group from MPA binds covalently with titania showing S-Ti bonds. PEG polymerized due to the several hydroxyl groups available for derivatization that crosslinked with each other forming multilayers. Further study will be needed to identify if APPA and MPA molecules formed monolayers or multilayers on the TiO_2 surface.

In conclusion, this study would be useful for the development of nanostructured TiO_2 films. It can also be used to better understand the adhesion mechanism of bifunctional molecules that can modify the physicochemical properties of the titania surface, thus opening a wide range of possible applications for these functional materials.

Acknowledgements

We would like to thank FAPESP [2014/01713-3; 2014/27015-0; 2014/20471-0], CEPID [2013/07296-2], NIH grant [DE 11657] and the Brodie Endowment Fund for providing financial support. The authors acknowledge Dr. Elidiane Cipriano Rangel and Dr. Marcelo Orlandi for the contact angle and SEM measurements, respectively.

Appendix A. Supplementary data

Supplementary material related to this article can be found, in the online version, at doi:https://doi.org/10.1016/j.colsurfa.2018.03.019.

References

[1] All-solid-state dye-sensitized solar cells with high efficiency : Nature : Nature Publishing Group, (n.d.). http://www.nature.com/nature/journal/v485/n7399/full/nature11067.html (Accessed 24 March 2016).
[2] S. Ito, P. Chen, P. Comte, M.K. Nazeeruddin, P. Liska, P. Péchy, M. Grätzel,

Fabrication of screen-printing pastes from TiO2 powders for dye-sensitised solar cells, Prog. Photovolt. Res. Appl. 15 (2007) 603–612, http://dx.doi.org/10.1002/pip.768.
[3] H.-H. Huang, S.-J. Pan, Y.-L. Lai, T.-H. Lee, C.-C. Chen, F.-H. Lu, Osteoblast-like cell initial adhesion onto a network-structured titanium oxide layer, Scr. Mater. 51 (2004) 1017–1021, http://dx.doi.org/10.1016/j.scriptamat.2004.08.017.
[4] F.G. Oliveira, A.R. Ribeiro, G. Perez, B.S. Archanjo, C.P. Gouvea, J.R. Araújo, A.P.C. Campos, A. Kuznetsov, C.M. Almeida, M.M. Maru, C.A. Achete, P. Ponthiaux, J.-P. Celis, L.A. Rocha, Understanding growth mechanisms and tribocorrosion behaviour of porous TiO2 anodic films containing calcium, phosphorous and magnesium, Appl. Surf. Sci. 341 (2015) 1–12, http://dx.doi.org/10.1016/j.apsusc.2015.02.163.
[5] M. Lilja, J. Forsgren, K. Welch, M. Åstrand, H. Engqvist, M. Strømme, Photocatalytic and antimicrobial properties of surgical implant coatings of titanium dioxide deposited though cathodic arc evaporation, Biotechnol. Lett. 34 (2012) 2299–2305, http://dx.doi.org/10.1007/s10529-012-1040-2.
[6] K. Nakata, A. Fujishima, TiO2 photocatalysis: Design and applications, J. Photochem. Photobiol. C Photochem. Rev. 13 (2012) 169–189, http://dx.doi.org/10.1016/j.jphotochemrev.2012.06.001.
[7] X. Chen, S.S. Mao, Titanium dioxide nanomaterials: synthesis, properties, modifications, and applications, Chem. Rev. 107 (2007) 2891–2959, http://dx.doi.org/10.1021/cr0500535.
[8] B.R. Sankapal, M.C. Lux-Steiner, A. Ennaoui, Synthesis and characterization of anatase-TiO2 thin films, Appl. Surf. Sci. 239 (2005) 165–170, http://dx.doi.org/10.1016/j.apsusc.2004.05.142.
[9] X. Wang, F. Shi, X. Gao, C. Fan, W. Huang, X. Feng, A sol–gel dip/spin coating method to prepare titanium oxide films, Thin Solid Films. 548 (2013) 34–39, http://dx.doi.org/10.1016/j.tsf.2013.08.056.
[10] Review on Sol-Gel Derived Coatings: Process, Techniques and Optical Applications, (n.d.). http://www.jmst.org/EN/abstract/abstract7092.shtml (Accessed 25 March 2016).
[11] M. Răileanu, M. Crişan, I. Niţoi, A. Ianculescu, P. Oancea, D. Crişan, L. Todan, TiO2-based Nanomaterials with Photocatalytic Properties for the Advanced Degradation of Xenobiotic Compounds from Water. A Literature Survey, Water. Air. Soil Pollut. 224 (2013), http://dx.doi.org/10.1007/s11270-013-1548-7.
[12] D. Vorkapic, T. Matsoukas, Effect of Temperature and Alcohols in the Preparation of Titania Nanoparticles from Alkoxides, J. Am. Ceram. Soc. 81 (1998) 2815–2820, http://dx.doi.org/10.1111/j.1151-2916.1998.tb02701.x.
[13] G. Oskam, A. Nellore, R.L. Penn, P.C. Searson, The Growth Kinetics of TiO2 Nanoparticles from Titanium(IV) Alkoxide at High Water/Titanium Ratio, J. Phys. Chem. B. 107 (2003) 1734–1738, http://dx.doi.org/10.1021/jp021237f.
[14] M. Sakeye, J.-H. Smått, Comparison of Different Amino-Functionalization Procedures on a Selection of Metal Oxide Microparticles: Degree of Modification and Hydrolytic Stability, Langmuir. 28 (2012) 16941–16950, http://dx.doi.org/10.1021/la303925x.
[15] K.M. Park, K.D. Park, Facile surface immobilization of cell adhesive peptide onto TiO2 substrate via tyrosinase-catalyzed oxidative reaction, J. Mater. Chem. 21 (2011) 15906, http://dx.doi.org/10.1039/c1jm13869c.
[16] C. Sanchez, C. Boissière, D. Grosso, C. Laberty, L. Nicole, Design, Synthesis, and Properties of Inorganic and Hybrid Thin Films Having Periodically Organized Nanoporosity, Chem. Mater. 20 (2008) 682–737, http://dx.doi.org/10.1021/cm702100t.
[17] M.S. Mozumder, A. Mairpady, A.-H.I. Mourad, Polymeric nanobiocomposites for biomedical applications: polymeric nanobiocomposites, J. Biomed. Mater. Res. B Appl. Biomater. (2016), http://dx.doi.org/10.1002/jbm.b.33633 n/a-n/a.
[18] E.V. Skorb, D.V. Andreeva, Surface Nanoarchitecture for Bio-Applications: Self-Regulating Intelligent Interfaces, Adv. Funct. Mater. 23 (2013) 4483–4506, http://dx.doi.org/10.1002/adfm.201203884.
[19] J. Massin, L. Ducasse, T. Toupance, C. Olivier, Tetrazole as a New Anchoring Group for the Functionalization of TiO2 Nanoparticles: A Joint Experimental and Theoretical Study, J. Phys. Chem. C. 118 (2014) 10677–10685, http://dx.doi.org/10.1021/jp502488g.
[20] S.P. Pujari, L. Scheres, A.T.M. Marcelis, H. Zuilhof, Covalent Surface Modification of Oxide Surfaces, Angew. Chem. Int. Ed. 53 (2014) 6322–6356, http://dx.doi.org/10.1002/anie.201306709.
[21] J.C. Love, L.A. Estroff, J.K. Kriebel, R.G. Nuzzo, G.M. Whitesides, Self-assembled monolayers of thiolates on metals as a form of nanotechnology, Chem. Rev. 105 (2005) 1103–1169, http://dx.doi.org/10.1021/cr0300789.
[22] F. Gao, A.V. Teplyakov, Challenges and opportunities in chemical functionalization of semiconductor surfaces, Appl. Surf. Sci. 399 (2017) 375–386, http://dx.doi.org/10.1016/j.apsusc.2016.12.083.
[23] R.L. McCreery, A.J. Bergren, Surface Functionalization in the Nanoscale Domain, in: M. Stepanova, in: S. Dew (Ed.), Nanofabrication, Springer Vienna, 2012, pp. 163–190, , http://dx.doi.org/10.1007/978-3-7091-0424-8_7.
[24] D. Brovelli, G. Hähner, L. Ruiz, R. Hofer, G. Kraus, A. Waldner, J. Schlösser, P. Oroszlan, M. Ehrat, N.D. Spencer, Highly Oriented, Self-Assembled Alkanephosphate Monolayers on Tantalum(V) Oxide Surfaces, Langmuir. 15 (1999) 4324–4327, http://dx.doi.org/10.1021/la981758n.
[25] F.K. Hansen, G. Rødsrud, Surface tension by pendant drop: I. A fast standard instrument using computer image analysis, J. Colloid Interface Sci. 141 (1991) 1–9, http://dx.doi.org/10.1016/0021-9797(91)90296-K.
[26] N. Ghows, M.H. Entezari, Ultrasound with low intensity assisted the synthesis of nanocrystalline TiO2 without calcination, Ultrason. Sonochem. 17 (2010) 878–883, http://dx.doi.org/10.1016/j.ultsonch.2010.03.010.
[27] J. Livage, M. Henry, C. Sanchez, Sol-gel chemistry of transition metal oxides, Prog. Solid State Chem. 18 (1988) 259–341, http://dx.doi.org/10.1016/0079-6786(88)90005-2.
[28] S.A. Alves, R. Bayón, V.S. de Viteri, M.P. Garcia, A. Igartua, M.H. Fernandes, L.A. Rocha, Tribocorrosion Behavior of Calcium- and Phosphorous-Enriched Titanium Oxide Films and Study of Osteoblast Interactions for Dental Implants, J. Bio- Tribo-Corros. 1 (2015) 1–21, http://dx.doi.org/10.1007/s40735-015-0023-y.
[29] G. Jakša, B. Štefane, J. Kovač, Influence of different solvents on the morphology of APTMS-modified silicon surfaces, Appl. Surf. Sci. 315 (2014) 516–522, http://dx.doi.org/10.1016/j.apsusc.2014.05.157.
[30] Poly(Ethylene Glycol) Chemistry - Biotechnical and | J. Milton Harris | Springer, (n.d.). http://www.springer.com/la/book/9780306440786 (Accessed 27 September 2017).
[31] A. Papra, N. Gadegaard, N.B. Larsen, Characterization of Ultrathin Poly(ethylene glycol) Monolayers on Silicon Substrates, Langmuir. 17 (2001) 1457–1460, http://dx.doi.org/10.1021/la000609d.
[32] K. Cai, M. Frant, J. Bossert, G. Hildebrand, K. Liefeith, K.D. Jandt, Surface functionalized titanium thin films: Zeta-potential, protein adsorption and cell proliferation, Colloids Surf. B Biointerfaces. 50 (2006) 1–8, http://dx.doi.org/10.1016/j.colsurfb.2006.03.016.
[33] G. Zhao, Z. Schwartz, M. Wieland, F. Rupp, J. Geis-Gerstorfer, D.L. Cochran, B.D. Boyan, High surface energy enhances cell response to titanium substrate microstructure, J. Biomed. Mater. Res. A. 74 (2005) 49–58, http://dx.doi.org/10.1002/jbm.a.30320.
[34] K.J. Kubiak, M.C.T. Wilson, T.G. Mathia, P. Carval, Wettability versus roughness of engineering surfaces, Wear. 271 (2011) 523–528, http://dx.doi.org/10.1016/j.wear.2010.03.029.
[35] D. Quéré, Wetting and Roughness, Annu. Rev. Mater. Res. 38 (2008) 71–99, http://dx.doi.org/10.1146/annurev.matsci.38.060407.132434.
[36] J.I. Rosales-Leal, M.A. Rodríguez-Valverde, G. Mazzaglia, P.J. Ramón-Torregrosa, L. Díaz-Rodríguez, O. García-Martínez, M. Vallecillo-Capilla, C. Ruiz, M.A. Cabrerizo-Vílchez, Effect of roughness, wettability and morphology of engineered titanium surfaces on osteoblast-like cell adhesion, Colloids Surf, Physicochem. Eng. Asp. 365 (2010) 222–229, http://dx.doi.org/10.1016/j.colsurfa.2009.12.017.
[37] S. Shin, J. Seo, H. Han, S. Kang, H. Kim, T. Lee, Bio-Inspired Extreme Wetting Surfaces for Biomedical Applications, Materials. 9 (2016) 116, http://dx.doi.org/10.3390/ma9020116.
[38] M.S. Mozumder, H. Zhang, J. Zhu, Mimicking Lotus Leaf: Development of Micro-Nanostructured Biomimetic Superhydrophobic Polymeric Surfaces by Ultrafine Powder Coating Technology, Macromol. Mater. Eng. 296 (2011) 929–936, http://dx.doi.org/10.1002/mame.201100080.
[39] R.N. Wenzel, Resistance of solid surfaces to wetting by water, Ind. Eng. Chem. 28 (1936) 988–994, http://dx.doi.org/10.1021/ie50320a024.
[40] J.F. Moulder, Handbook of X-ray Photoelectron Spectroscopy: A Reference Book of Standard Spectra for Identification and Interpretation of XPS Data, Physical Electronics Division, Perkin-Elmer Corporation, 1992.
[41] M. Shahnas Beegam, S.B. Narendranath, P. Periyat, Tuning of selective solar photocatalysis by Mn2+ decorated nanocrystalline mesoporous TiO2, Sol. Energy. 158 (2017) 774–781, http://dx.doi.org/10.1016/j.solener.2017.10.046.
[42] B. Shi, H. Yin, J. Gong, Q. Nie, A novel p-n heterojunction of Ag2O/Bi4Ti3O12 nanosheet with exposed (001) facets for enhanced visible-light-driven photocatalytic activity, Mater. Lett. 201 (2017) 74–77, http://dx.doi.org/10.1016/j.matlet.2017.04.146.
[43] M. Zafar, J.-Y. Yun, D.-H. Kim, Performance of inverted organic photovoltaic cells with nitrogen doped TiO_2 films by atomic layer deposition, Korean J. Chem. Eng. (2017) 1–7, http://dx.doi.org/10.1007/s11814-017-0285-9.
[44] Y.-Y. Song, H. Hildebrand, P. Schmuki, Optimized monolayer grafting of 3-aminopropyltriethoxysilane onto amorphous, anatase and rutile TiO2, Surf. Sci. 604 (2010) 346–353, http://dx.doi.org/10.1016/j.susc.2009.11.027.
[45] V. Paredes, E. Salvagni, E. Rodríguez-Castellon, F.J. Gil, J.M. Manero, Study on the use of 3-aminopropyltriethoxysilane and 3-chloropropyltriethoxysilane to surface biochemical modification of a novel low elastic modulus Ti–Nb–Hf alloy, J. Biomed. Mater. Res. B Appl. Biomater. 103 (2015) 495–502, http://dx.doi.org/10.1002/jbm.b.33226.
[46] G.J. Fleming, K. Adib, J.A. Rodriguez, M.A. Barteau, J.M. White, H. Idriss, The adsorption and reactions of the amino acid proline on rutile TiO2(110) surfaces, Surf. Sci. 602 (2008) 2029–2038, http://dx.doi.org/10.1016/j.susc.2008.04.010.
[47] J.N. Wilson, R.M. Dowler, H. Idriss, Adsorption and reaction of glycine on the rutile TiO2(011) single crystal surface, Surf. Sci. 605 (2011) 206–213, http://dx.doi.org/10.1016/j.susc.2010.10.020.
[48] E. Ataman, C. Isvoranu, J. Knudsen, K. Schulte, J.N. Andersen, J. Schnadt, Adsorption of L-cysteine on rutile TiO2(110), Surf. Sci. 605 (2011) 179–186, http://dx.doi.org/10.1016/j.susc.2010.10.017.
[49] K.I. Maslakov, Y.A. Teterin, A.J. Popel, A.Y. Teterin, K.E. Ivanov, S.N. Kalmykov, V.G. Petrov, R. Springell, T.B. Scott, I. Farnan, XPS study of the surface chemistry of UO2 (111) single crystal film, Appl. Surf. Sci. 433 (2018) 582–588, http://dx.doi.org/10.1016/j.apsusc.2017.10.019.
[50] T. Hanawa, A comprehensive review of techniques for biofunctionalization of titanium, J. Periodontal Implant Sci. 41 (2011) 263–272, http://dx.doi.org/10.5051/jpis.2011.41.6.263.
[51] K.J.A. Raj, R. Shanmugam, R. Mahalakshmi, B. Viswanathan, XPS and IR spectral studies on the structure of phosphate and sulphate modified titania – a combined DFT and experimental study, IJC 49 (A01 January 2010) (2010) (Accessed 5 August 2016), http://nopr.niscair.res.in/handle/123456789/7185.
[52] H. Zhang, Z. Yang, X. Zhang, N. Mao, Photocatalytic effects of wool fibers modified with solely TiO2 nanoparticles and N-doped TiO2 nanoparticles by using hydrothermal method, Chem. Eng. J. 254 (2014) 106–114, http://dx.doi.org/10.1016/j.

cej.2014.05.097.
[53] C. Ketul, Sadhana Popat, Tejal A. Sharma, Desai, Quantitative XPS Analysis of PEG-Modified Silicon Surfaces, J Phys Chem B. 108 (2004) 5185–5188, http://dx.doi.org/10.1021/jp049260j.
[54] Functionalization Strategies for Protease Immobilization on Magnetic Nanoparticles - Li- 2010 - Advanced Functional Materials - Wiley Online Library, (n.d.). http://onlinelibrary-wiley-com.ez87.periodicos.capes.gov.br/doi/10.1002/adfm.201000188/full (Accessed 9 August 2016).
[55] E.J. Falde, S.T. Yohe, Y.L. Colson, M.W. Grinstaff, Superhydrophobic materials for biomedical applications, Biomaterials 104 (2016) 87–103, http://dx.doi.org/10.1016/j.biomaterials.2016.06.050.